processes

MDPI

Article

Influence of Graphene Nano Fillers and Carbon Nano Tubes on the Mechanical and Thermal Properties of Hollow Glass Microsphere Epoxy Composites

Kumar D [1], Kiran Shahapurkar [2,*], C. Venkatesh [2], Muruganandhan R [3], Vineet Tirth [4], Chandru Manivannan [5], Ibrahim M. Alarifi [6], Manzoore Elahi M. Soudagar [7] and Ahmed S. El-Shafay [8,9]

1 Department of Mechanical Engineering, C. Abdul Hakeem College of Engineering and Technology, Melvisharam 632509, Tamilnadu, India; ilayakumard@gmail.com
2 School of Mechanical, Chemical and Materials Engineering, Adama Science and Technology University, Adama 1888, Ethiopia; venkyachvsh@yahoo.co.in
3 Department of Mechanical Engineering, College of Engineering Guindy, Anna University, Chennai 600025, Tamilnadu, India; murugandesign@gmail.com
4 Mechanical Engineering Department, College of Engineering, King Khalid University, Abha 61421, Asir, Saudi Arabia; vtirth@kku.edu.sa
5 Department of Mechanical Engineering, Dhirajlal Gandhi College of Technology, Salem 636309, Tamilnadu, India; mechchandru123@gmail.com
6 Department of Mechanical and Industrial Engineering, College of Engineering, Majmaah University, Al-Majmaah 11952, Riyadh, Saudi Arabia; i.alarifi@mu.edu.sa
7 Department of Mechanical Engineering, School of Technology, Glocal University, Delhi-Yamunotri Marg, SH-57, Mirzapur Pole, Saharanpur 247121, India; me.soudagar@gmail.com
8 Department of Mechanical Engineering, College of Engineering, Prince Sattam bin Abdulaziz University, Alkharj 16273, Saudi Arabia; a.abdou@psau.edu.sa
9 Mechanical Power Engineering Department, Faculty of Engineering, Mansoura University, Mansoura 35516, Egypt
* Correspondence: kiranhs1588@astu.edu.et

Abstract: The present work aimed to analyze the roll of carbon nano tubes and graphene nano fillers on the mechanical and thermal characteristics of hollow glass microsphere reinforced epoxy composites. Composites with varying content of hollow glass microballoons (2, 4, 6, 8, and 10 wt %) reinforced in epoxy matrix were fabricated. Additionally, two more types of composites, one with graphene nano fillers and the other with carbon nano tube at a constant 0.5 wt %, were fabricated with varying weight percentages of hollow glass microballoons (2, 4, 6, 8, and 10%). The composites were fabricated using an open mold casting process. Composites were tested for thermal and mechanical properties. The tensile and flexural moduli were found to rise as the HGM concentration increased. Graphene-filled HGM/epoxy composites revealed the highest modulus compared with HGM/epoxy and HGM/CNT/epoxy composites. The impact strength of all composite types decreased as the HGM content increased. Neat epoxy specimens revealed low response as compared with all the composites tested. Further, the thermal conductivity of HGM/epoxy composites was lower as compared with other compositions and neat epoxy. Scanning electron microscopy was used to analyze the surface morphological behavior of the composites subjected to flexural test. It was found that HGM/G/E composites with 10% of HGM and 0.5% of graphene by weight in epoxy matrix were the optimum.

Keywords: epoxy; hollow glass microsphere; nano fillers; carbon nano tube; graphene; mechanical and thermal properties

check for updates

Citation: D, K.; Shahapurkar, K.; Venkatesh, C.; R, M.; Tirth, V.; Manivannan, C.; Alarifi, I.M.; Soudagar, M.E.M.; El-Shafay, A.S. Influence of Graphene Nano Fillers and Carbon Nano Tubes on the Mechanical and Thermal Properties of Hollow Glass Microsphere Epoxy Composites. *Processes* **2022**, *10*, 40. https://doi.org/10.3390/pr10010040

Academic Editor: Jayantha Epaarachchi

Received: 15 November 2021
Accepted: 8 December 2021
Published: 27 December 2021

Publisher's Note: MDPI stays neutral with regard to jurisdictional claims in published maps and institutional affiliations.

Copyright: © 2021 by the authors. Licensee MDPI, Basel, Switzerland. This article is an open access article distributed under the terms and conditions of the Creative Commons Attribution (CC BY) license (https://creativecommons.org/licenses/by/4.0/).

1. Introduction

Closed cell hollow particles are reinforced in matrix to realize syntactic foams [1–3]. These foams offer advantages of lower moisture inclusion, high compression response,

and higher damage tolerances [4,5]. High flexibility in design can be attained by selecting suitable hollow spheres and matrices. These hollow particles are widely employed with polymer matrix composites because they are lightweight, have a high strength-to-weight ratio, and are stiff [6]. They are widely used in a variety of industries, including electrical, aerospace, marine, automotive, and sports, among others [7]. Ferreira et al. examined the influence of HGM filler with carbon short fiber and glass-reinforced epoxy composites and found that with the increase of HGM content, there was an increase in flexural, compressive, and impact properties. The carbon content increased flexural and fracture toughness properties, and the glass fiber content increased impact properties, while hybrid composites did not improve the impact properties [8]. Mohammed Imran et al. have investigated the effect of compressive strength of carbon nanofibers grown on HGM epoxy composite foam and observed that the compressive strength increased, owing to the high modulus of carbon nano-materials. The carbon nanofibers grown at 500 °C were of solid graphite structure, and those grown at 600 °C and 700 °C were of hollow graphite structure [9]. Koopman et al. explored the compression of glass micro balloons and observed a clear correlation between the diameter to failure load and diameter to fracture energy [10]. Mohammed Imran et al. studied the variable weight percentage of HGM in epoxy composites made by the sonication method and reported that the compressive strength declined when the HGM weight percentage increased and the storage modulus increased [11]. Rahaman et al. investigated the glass fiber-reinforced laminated epoxy carbon nano tube composites and discovered that the addition of multi-walled carbon nano tubes significantly enhanced the composite's flexural modulus, flexural strength, and modulus of storage [12]. Ho Sung Kim et al. examined the impact and fracture properties on the HGM/epoxy composites and observed that the HGM did not enhance the fracture toughness, impact force, and specific flexural strength while the flexural modulus was increased [13]. An investigation of the dielectric properties of HGM/epoxy composites was conducted by Yung et al., observing that as the HGM content increased, the dielectric constant, dielectric loss, and thermal conductivity were reduced. With an increase in HGM content, the thermal expansion coefficient and glass transition temperature improved [14]. Swetha et al. performed an experiment to study the mechanical characteristics of HGM/epoxy composites and observed that the modulus and strength decreased with increasing HGM volume percent but improved with increasing microsphere wall thickness [15]. Yingjie Qiao et al. studied the compression and thermal characteristics of the HGM/epoxy composites, observing that the density, compressive modulus, compressive strength, and thermal conduction property of the composites decreased as the HGM volume percentage increased [16]. Mohammed Imran et al. studied the characteristics of HGM and CNT reinforced epoxy composites and observed that the compressive strength increased up to 5 weight percentage of HGM and decreased thereafter. The modulus of storage of the composites rose as HGM concentration increased [17]. Ronald et al. analyzed the water immersion properties of the carbon nanofiber reinforced epoxy composites with glass micro balloons and found that the compression modulus was not affected but decreased the compression strength [18]. Tien et al. investigated the influence of volume percentage and wall thickness of glass micro balloon reinforced epoxy matrix syntactic foams. According to their findings, the glass transition temperature rose as the volume percentage increased and was not affected by wall thickness, whereas thermal stability increased with increased wall thickness and was not affected by volume fraction [19]. CNT and graphene fillers in reinforced polymer nanocomposites were studied by Garima Mittal et al. They determined that increasing the filler loading reduced the electrical and mechanical characteristics of the material, owing to particle agglomeration. Additionally, CNT-based composites had lower load transfer and electrical conductivity than graphene-based composites [20]. Nishant Shirodkar et al. studied the graphene/epoxy nano-composites and observed that small quantity addition of graphene powder and proper mixing had an effect on the polymer's mechanical characteristics [21]. Dong Ho Kang et al. explored the influence of HGM on the single-walled carbon nano tube-loaded polypropylene composites, observing that 1~7 weight percentage

of HGM showed better performance [22]. Xin Zhao et al. examined the mechanical characteristics of graphene-based polyvinyl alcohol composites, finding that the mechanical characteristics were optimum at 1.8 volume percentage of graphene [23]. Mohammad A. Rafiee et al. investigated the mechanical characteristics of epoxy nanocomposite reinforced with graphene as well as single-walled and multi-walled carbon nano tubes, observing that the graphene performed better than graphene CNT additives [24]. Shao-Yun Fu et al. observed that the toughness and strength of particulate polymer matrix composites were influenced by particle/matrix adhesion, particle size, and particle content, while composite stiffness was found to be determined by particle content rather than particle/matrix adhesion [25]. Very few studies are available on the comparative studies on the influence of CNT and graphene nano fillers on thermal and mechanical characteristics of HGM reinforced epoxy composites [26,27].

This work aimed to examine the comparative effect of CNT and graphene nano fillers on thermal and mechanical properties with varying weight percentages of HGM reinforced epoxy composites. Epoxies are used as structural adhesives and matrix materials because they are inexpensive, easy to fabricate, have high specific strength, and provide thermal and electrical insulation. HGM is an emerging material that influences the properties even for small concentrations and is preferred where there is a need to combine high Young's modulus with low density. CNTs are important fillers due to their nanoscale dimensions and exceptional mechanical, thermal, and electrical properties. Another excellent filler material is graphene, a carbon allotrope made of a monolayer of carbon atoms organized in a 2D (two-dimensional) hexagonal lattice nanostructure with one atom forming each vertex. It has a high surface area and robust mechanical and electrochemical properties used in composites, electronics, energy, and biomedical fields.

Composites were prepared using varying amounts of hollow glass micro balloons (0, 2, 4, 6, 8, and 10 wt %) in epoxy matrix by using open mold casting. The novel aspects of the present study include (a) use of hollow glass micro balloons, CNT, and graphene for developing polymer composites; (b) the effect of varying hollow glass micro balloons on the mechanical and thermal properties; and (c) structure-property correlations for varying amounts of filler content.

2. Experimental Work

2.1. Materials

Araldite LY 556 Epoxy resin and Aradur HY 951 hardener were procured from Huntsman Advanced Materials India Private Limited, Mumbai, India. Cured epoxy resin and hardener has a density of 1.19 g/cm^3, tensile strength of 52 MPa, tensile modulus of 2800 MPa, elongation at break of 11%, shear modulus of 1230 MPa, Shore D hardness of 85, and glass transition temperature of 67 °C. Hollow glass microspheres with trade name MicroLite GM 20 made of soda-lime borosilicate glass were procured from Petra Buildcare Products, Bhavnagar, Gujarat, India. Hollow glass microspheres have a particle size of 2–13 μm, true density of 0.18–0.22 g/cm^3, and thermal conductivity of 0.0521 W/mK at 20 °C. Carbon nano tube and graphene were obtained from Sigma-Aldrich Chemicals Private Limited, Bangalore, India. Carbon nano tubes (CNTs) are the allotrope of carbon and are cylindrical in shape with an average particle size of <50 nm, tube length of 5 to 30 nanometer, true density of 2.26 g/cm^3, and specific surface area of 50 to 500 m^2/g. Graphene, a promising carbon nanomaterial, has an atomically thin single-layer structure. Surface area of graphene > 500 m^2/g and electrical conductivity of graphene $\geq$ 1000 S/m.

2.2. Specimen Preparation

The composites were prepared using the open mold casting process. Composites with hollow glass microspheres in varying content (2, 4, 6, 8, and 10 wt %) were prepared by thoroughly mixing with epoxy resin (Araldite LY556) and finally with the hardener (Aradur HY 951) in the resin: hardener ratio of 100:10 by weight. The prepared mixture was poured into two sets of molds, first with dimensions of 110 mm diameter with 5 mm

thickness, and second with 180 × 180 × 6 mm. Molds were applied with releasing agent before pouring of the mixture and cured at the atmospheric condition for 24 h. The samples removed from the mold were marked and cured in a hot air oven at 70 °C for 4 h. For comparative studies, a similar procedure was repeated for the fabrication of hollow glass microsphere-filled epoxy composites with varying weight percentages (2%, 4%, 6%, 8%, and 10%) and CNTs (constant 0.5% by weight) and graphene (constant 0.5% by weight) separately. The disc-shaped specimens from the first mold were used for thermal properties, while the specimens marked and cut from plate-shaped composites were used for evaluating mechanical properties. Figure 1 shows the flow diagram of composite fabrication. Figure 2a,b shows the photographs of dies used for sample preparation of mechanical and thermal properties respectively. Figure 3 shows the photographs of specimens of (i) tensile, (ii) flexural, (iii) impact and (iv) thermal conductivity. Figure 3a shows the specimens of Hollow Glass Microspheres reinforced Epoxy (HGM/E) composites. Figure 3b shows the specimens of Hollow Glass Microspheres and Carbon Nano Tubes reinforced Epoxy (HGM/CNT/E) composites. Figure 3c shows the specimens of Hollow Glass Microspheres and Graphene reinforced Epoxy (HGM/G/E) composites.

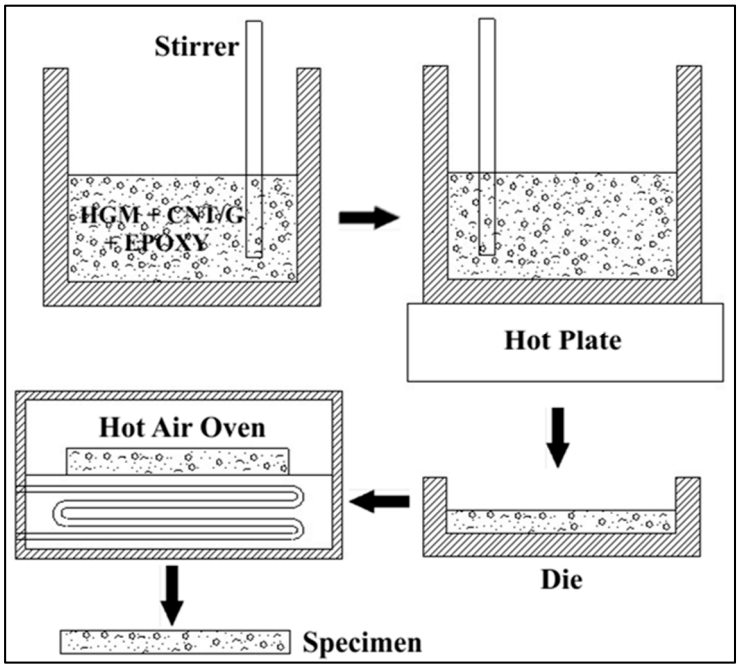


Figure 1. Flow diagram of composite fabrication.

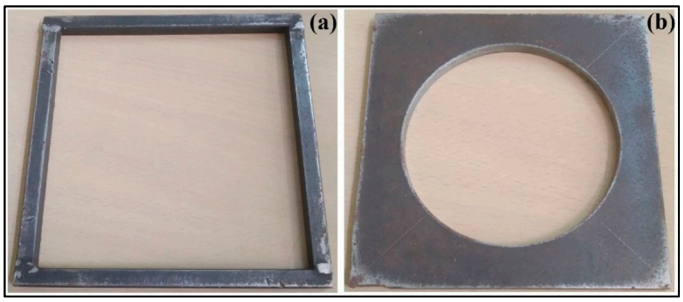


Figure 2. Photographs of dies used for sample preparation: (**a**) mechanical and (**b**) thermal.

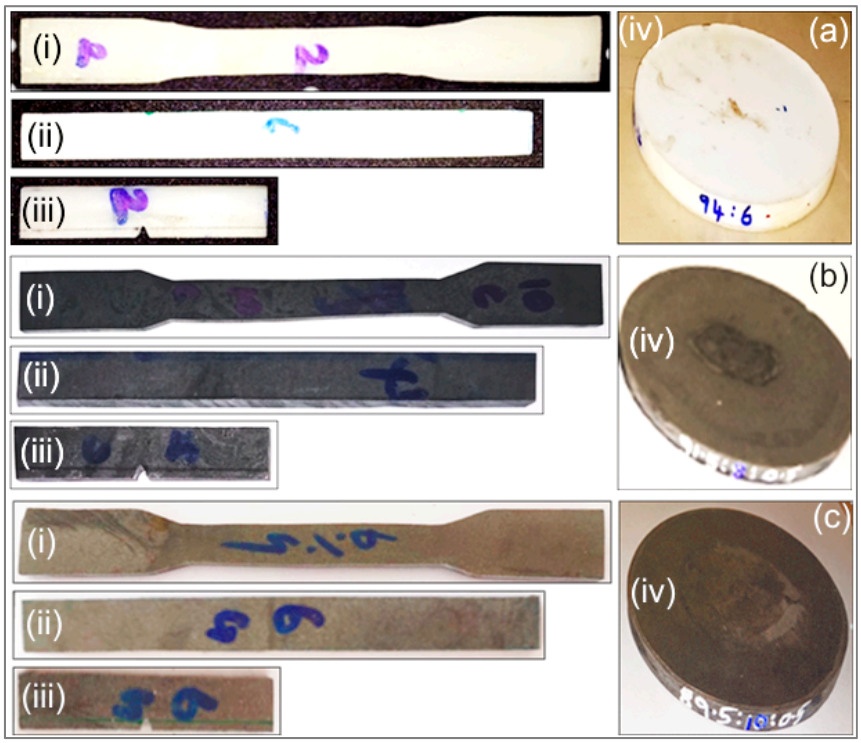


Figure 3. Photographs of specimens: (**a**) HGM/E composites, (**b**) HGM/CNT/E composites, and (**c**) HGM/G/E composites; (**i**) tensile, (**ii**) flexural, (**iii**) impact, and (**iv**) thermal conductivity.

Theoretical density (ρ^{th}) is calculated using the mixing rule and is represented by

$$\rho^{th} = \rho_f V_f + \rho_m V_m \tag{1}$$

where

ρ^{th}—theoretical density;
ρ_f—density of filler;
V_f—filler volume fraction;
ρ_m—density of matrix;
V_m—matrix volume fraction.

Additionally, the experimental density (ρ^{th}) is determined using the Archimedes principle by measuring mass of samples in air and water. Estimation of the void content ($\varnothing_V$) is accomplished by comparing experimental and theoretical density values and is denoted by

$$\varnothing_V = \frac{\left(\rho^{th} - \rho^{exp}\right)}{\rho^{exp}} \tag{2}$$

where

$\varnothing_V$—void content;
ρ^{th},ρ^{exp}—theoretical and experimental density values, respectively.

2.3. Tensile, Flexural, Impact, and Thermal Conductivity

To investigate the mechanical behavior of composites, we conducted tensile, impact, and flexural tests on all the specimens. The specimens for these tests were cut from the composites molded in the form of a plate. Tensile tests were performed on specimens of 165 × 12.7 × 3 mm with a gauge length of 115 mm conforming to ASTM D638 standard. Shimadzu (AG-50kNISD MS, Kyoto, Japan) universal testing machine was employed to

conduct tensile tests at a 50 mm/min cross-head speed. The dog bone-shaped specimen was clamped between the cross heads and loaded using the moving cross head until themaximum load was reached. From the observed load and elongation values, we calculated the tensile properties. Flexural tests were performed on specimens of size 127 × 12.7 × 3 mm as per ASTM D790 standards. Three-point bending flexural test was carried out on an Instron (3382, Boston, MA, USA) universal testing machine with 2.6 mm/min cross-head speed for 130 mm span length. The specimen was kept between supports and loaded using the moving cross-head until the yield was reached. From the observed load and deflection values, we calculated the flexural properties. Impact tests were performed on specimens of size 63.5 × 12.7 × 3 mm with a V-notch as per ASTM D256 standards. Izod impact test with 2.54 mm "V" notch depth and 45° notch angle was performed on a Tinius Olsen (IT 504, Horsham, PA, USA) impact testing machine. The notched specimen was fixed vertically in the impact testing machine vice and broken with a swinging pendulum. The amount of energy absorbed by the material during the breaking process was directly noted from the machine. To study the thermal behavior, we performed the thermal conductivity test on disc-shaped specimens of sizes of 110 mm diameter with 5 mm thickness using Lee's disc apparatus. The specimen was kept on the horizontally suspended disc, and steam was passed into the steam chamber placed on the specimen until the temperatures in the chamber and the disc were steady. The temperatures of the steam chamber and disc were noted. Then, the specimen was removed, and the steam chamber was placed directly on the disc. The disc was heated at 5 °C above the temperature of the disc. The steam chamber was removed, and the disc alone was allowed to cool. The temperature of the disc while cooling was noted at regular intervals. A graph was drawn between temperature and time, and slope at the steady temperature was obtained. Thermal conductivity was calculated from these graphs.

2.4. Scanning Electron Microscopy

Structure-property correlations of flexural fracture surfaces were carried out using scanning electron microscopy. A field emission scanning electron microscope (FESEM) FEI, Quanta 200 was employed for imaging the surfaces. The fractured portion of the specimens was cut to a height of 10 mm without disturbing the fractured surface. Gold palladium electroplating was used to coat fractured surfaces to prevent electron charging. The coated samples were attached to a stub by double-sided electrically conductive adhesive carbon tape. An accelerating voltage of 10 kV power supply was used for imaging the specimens.

3. Results and Discussion

3.1. Density

Method of fabrication, uniform dispersion of constituents in the epoxy matrix, and lower void content significantly influenced the mechanical behavior of composites. Experimentally measured densities of different composites are depicted in Figure 4. Further, void content estimations, as well as theoretical and experimental density, are reported in Table 1. Experimental density values were lower than theoretical density values due to the entrapment of air in the composite encountered during fabrication. However, it was evident that the densities of all the composites declined with increasing hollow glass microballoon content. Hollow glass microballoons have an average density of 200 kg/m^3, which is lower than neat epoxy by roughly six times. These microballoons, apart from possessing low density, are also hollow in nature; thereby, more space is utilized by the fillers in the composite. As a result, all the composites revealed a decrease in density values as the HGM content increased. Similar trends can be observed in [14,28–30]. Furthermore, HGM/E composites revealed lower density as compared with HGM/CNT/E and HGM/G/E. Further, the void content estimations indicated that observed values were minimal and can be neglected. The minute variations noticed in the standard deviations affirmed the consistency achieved in the fabrication of samples.

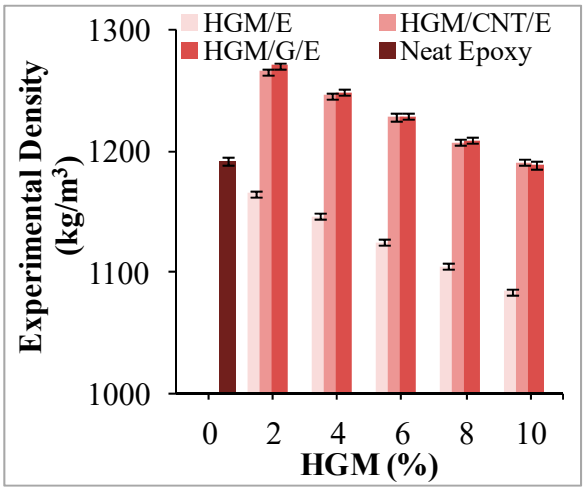


Figure 4. Experimental measured density of different composites.

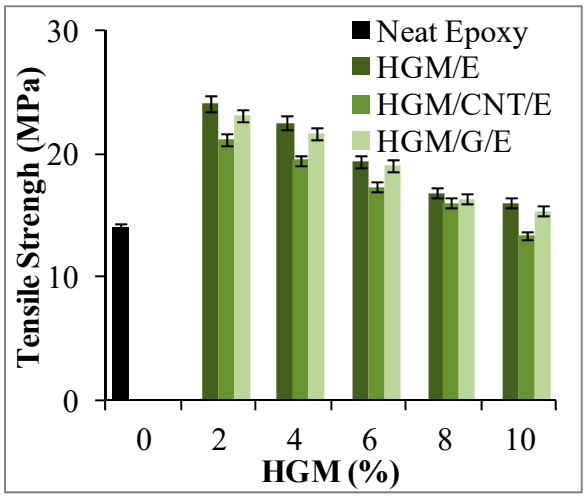
Table 1. Density and void content estimation of specimens.

Specimen Designation	Material Composition HGM/CNT/G:E (Weight %)	Theoretical Density (ρ^{th}) (kg/m^3)	Experimental Density (ρ^{exp}) (kg/m^3)	Void Content (ϕ_V)
2HGM/E	2:0:0:98	1172.160	1165.300 ± 25.637	0.588
4HGM/E	4:0:0:96	1152.320	1146.450 ± 25.222	0.512
6HGM/E	6:0:0:94	1132.480	1124.600 ± 24.741	0.700
8HGM/E	8:0:0:92	1112.640	1104.540 ± 24.300	0.733
10HGM/E	10:0:0:90	1092.800	1084.440 ± 23.858	0.770
2HGM/CNT/E	2:0.5:0:97.5	1276.700	1265.420 ± 27.839	0.891
4HGM/CNT/E	4:0.5:0:95.5	1256.860	1245.650 ± 27.404	0.899
6HGM/CNT/E	6:0.5:0:93.5	1237.020	1228.250 ± 27.022	0.714
8HGM/CNT/E	8:0.5:0:91.5	1217.180	1207.320 ± 26.561	0.816
10HGM/CNT/E	10:0.5:0:89.5	1197.340	1190.350 ± 26.188	0.587
2HGM/G/E	2:0:0.5:97.5	1279.200	1270.230 ± 27.945	0.706
4HGM/G/E	4:0:0.5:95.5	1259.360	1248.630 ± 27.470	0.859
6HGM/G/E	6:0:0.5:93.5	1239.520	1228.450 ± 27.026	0.901
8HGM/G/E	8:0:0.5:91.5	1219.680	1208.660 ± 26.591	0.911
10HGM/G/E	10:0:0.5:89.5	1199.840	1188.450 ± 26.146	0.958

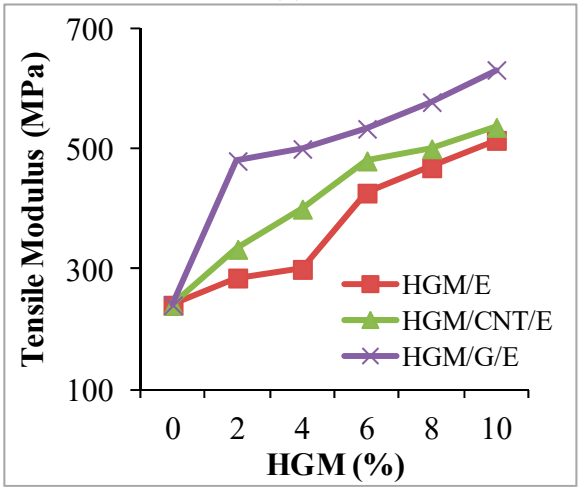
3.2. Tensile Strength and Modulus

The response of composites to resist applied forces in tension is vital since it provides information the materials to resist when forces are applied in tension. Determining the tensile properties is crucial because it provides information concerning various tensile properties (elastic limit, tensile strength, modulus of elasticity, etc.). Tensile properties vary for every composites, and thereby tensile tests are performed to understand the behavior of different composites [31]. Tensile strength and modulus of HGM/E, HGM/CNT/E, and HGM/G/E composites are depicted in Figure 5. The tensile strengths of different HGM composites are presented in Figure 5a. It is noticed that when the amount of HGM in the composites increased, the tensile strength of the composites fell. This was because tensile strength is governed by bonding strength, effective load transfer, particle size, and particle loading, primarily adhesion between particles and matrix [25,32–34]. As the particle loading rose, the compatibility between the matrix and particles was lost due to insufficient matrix material to cover the particles, and load transfer decreased, resulting in the reduction of tensile strength. Comparing the tensile strength of HGM/E, HGM/CNT/E, and HGM/G/E composites, we found that the effect of additional reinforcements (carbon nano tubes and graphene) did not yield a significant change in the strength of the composites.

Tensile modulus of HGM/E, HGM/CNT/E, and HGM/G/E composites are shown in Figure 5b. Contrary to the strength values, tensile modulus of all the composites depicted increasing trends with an increase in volume fraction of hollow glass microballoons. It is noted that the tensile modulus increased with an increase in reinforcing particle loading. This was because modulus depends on particle loading and not on particle/matrix adhesion, since the particles have a higher modulus than the matrix. Moreover, when the particles are nano-sized with a larger surface area, a nano effect is created that greatly enhances the stiffness. Comparing the tensile modulus of HGM/E, HGM/CNT/E, and HGM/G/E composites, we found that the addition of graphene resulted in the highest modulus yield when compared to carbon nano tubes, owing to their intrinsic mechanical characteristics and the strong interfacial bonding, which results in an improved interfacial stress transfer efficiency [35–37].



(**a**)



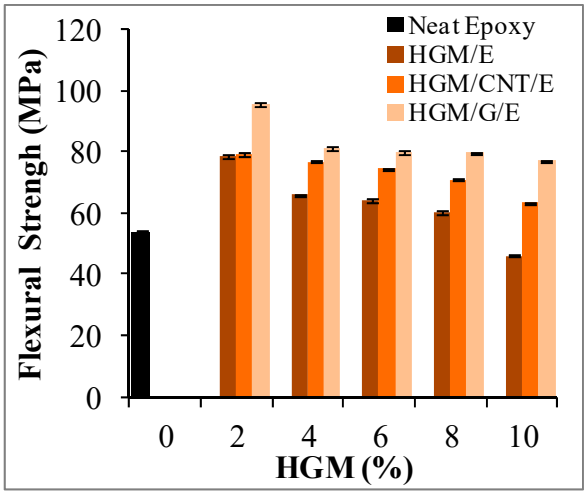
(**b**)

Figure 5. Tensile (**a**) modulus and (**b**) strength of composites.

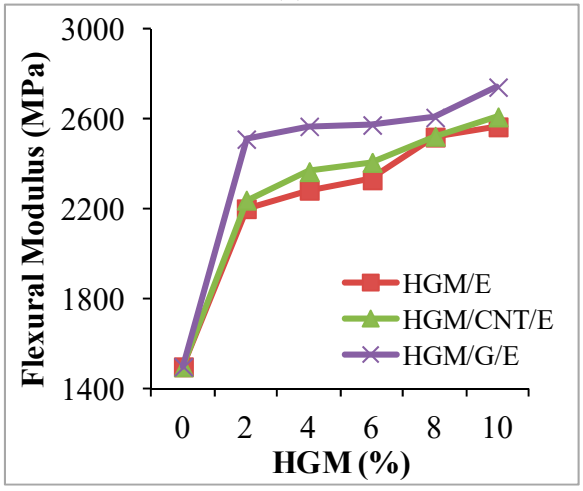
3.3. Flexural Strength and Modulus

Composites' ability to withstand bending deflection when subjected to various loads is termed as flexural strength. Composites designed for many products and applications require retention of flexural properties [38]. Figure 6a displays the flexural strength of HGM/E, HGM/CNT/E, and HGM/G/E composites. The strength of all the composites revealed trends similar to tensile behavior, wherein HGM/G/E depicted higher strength as compared with HGM/CNT/E and HGM/E. However, the strength of all the composites decreased with a rise in hollow glass microballoon content. Flexural modulus of HGM/E,

HGM/CNT/E, and HGM/G/E composites are shown in Figure 6b. Modulus of all the composites depicts increasing trends with an increase in hollow glass microballoon content. A significant rise in modulus was seen with HGM/G/E composites, owing to an exceptionally high aspect ratio and higher modulus of graphene particles that assist in good load transfer from the matrix to reinforcements, thereby enhancing the overall modulus [39]. Similar trends were reported by [40–42].



(**a**)



(**b**)

Figure 6. Flexural (**a**) strength and (**b**) modulus of composites.

3.4. Impact Strength

Composites' response to sudden impact loads is the crucial property required for most of the envisaged applications. Comparison of impact strength of HGM/E, HGM/CNT/E, and HGM/G/E composites is depicted in Figure 7. With the increase in HGM content, the impact strength of the composites decreased for all the composites. This was due to the fact that the increase of hard reinforcing particles increased brittleness and clustering and hence decreased the impact strength at higher particle loading.

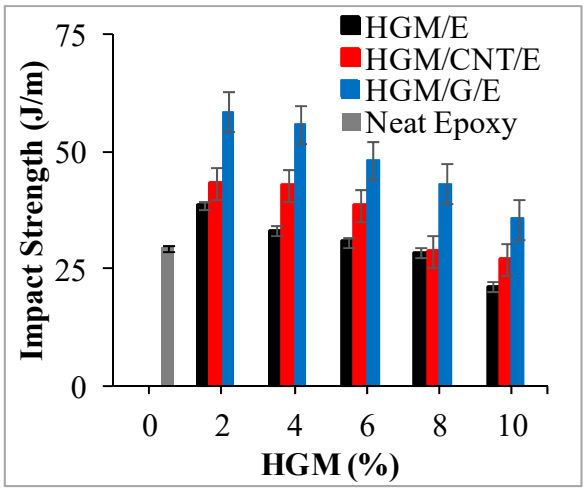


Figure 7. Impact strength of composites.

The addition of hard reinforcing particles increased brittleness and stress concentration points, and hence the strengths of the composites reduced with the increment in HGM weight percentage. On the other hand, HGM/G/E composites were found to have superior mechanical characteristics in comparison with the properties of HGM/CNT/E composites. This was because of the higher aspect ratio and two-dimensional plane structure of the graphene that transfers the load better within the matrix.

3.5. Thermal Conductivity

Thermal conductivity is an important property of composites designed for thermal applications. Low thermal conductivity of hollow glass microballoons and high aspect ratio of CNTs and graphene are beneficial in effectively building thermal networks [43]. Figure 8 compares the thermal conductivities of the HGM/E, HGM/CNT/E, and HGM/G/E composites. The thermal conductivity of all composites decreased with increasing HGM content. However, HGM/E composites revealed the lowest thermal conductivity as compared with HGM/CNT/E and HGM/G/E composites. The low thermal conductivity of HGM/E composites was mainly attributed to the ability of hollow glass microballoons to absorb moisture effectively. However, with the addition of CNT and graphene in the HGM/epoxy composites, the thermal conductivity increased by up to 4% by weight. This was because the thermal conductivity of graphene and CNT are higher than the thermal conductivity of HGM.

The present work effectively demonstrates the development of three different types of composites, namely, HGM/E, HGM/CNT/E, and HGM/G/E, with a purpose to widen the material options available for polymer-based composites. All the composites revealed good flexural properties and thermal conductivity with moderate impact strength. These composites can be utilized as core for preparation of sandwich composites and targeted for thermal applications. The composites can also be used in the fabrication of casing for energy storage devices and electronic equipment requiring dissipation of heat developed due to the chemical reaction or operation of electronic devices to the surrounding.

3.6. Micrography

Figure 9a–e shows the scanning electron microscopy images of flexural fractured surfaces of HGM/CNT/E composites with varying content of HGM from 0 to 10 wt %. It is evident from the micrographs that there was good dispersion of the reinforcing particles in the epoxy matrix. Further, it was also observed that clustering took place at the higher loading of HGM particles. Nevertheless, as the HGM content increased, survival of hollow particles also increased, and thereby there was an increase in the modulus of the composites at increasing HGM content. Under flexural loading, both compressive and tensile stresses

were developed in the composites. Striation marks can be seen on all the specimens, irrespective of HGM content; however, the magnitude of striations decreased with higher HGM content. As a result, the modulus of composites showed an increasing trend.

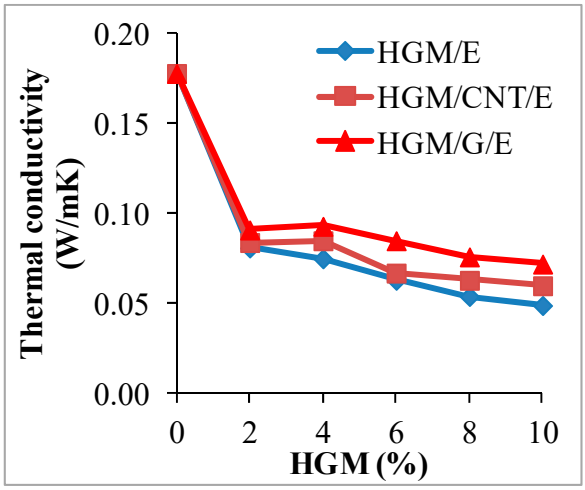


Figure 8. Thermal conductivity of composites.

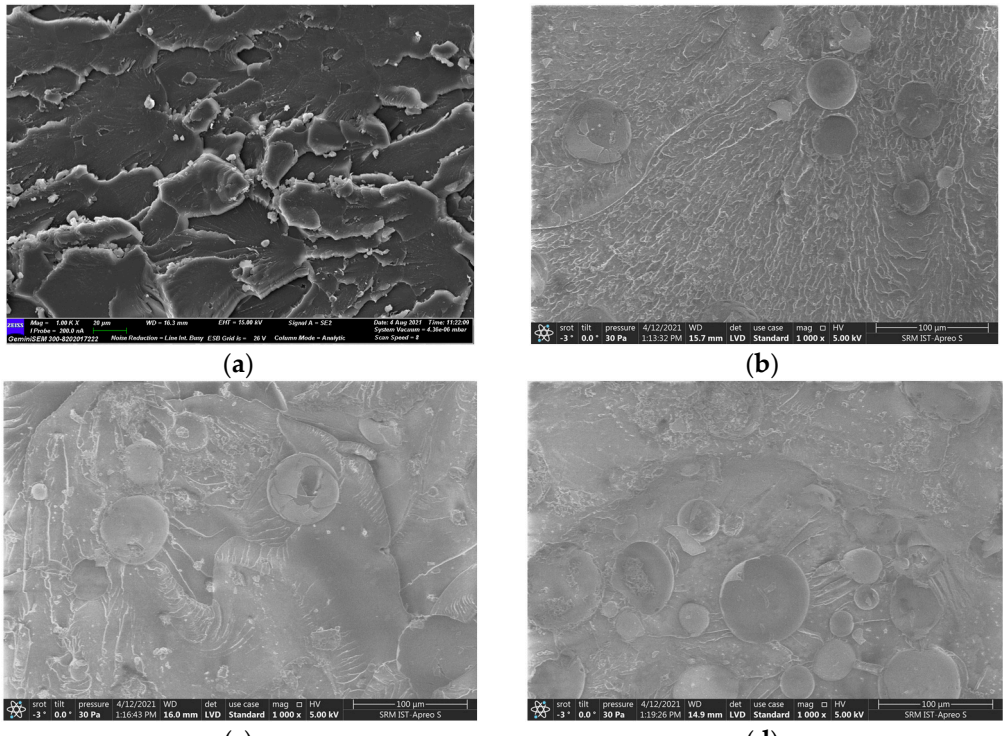
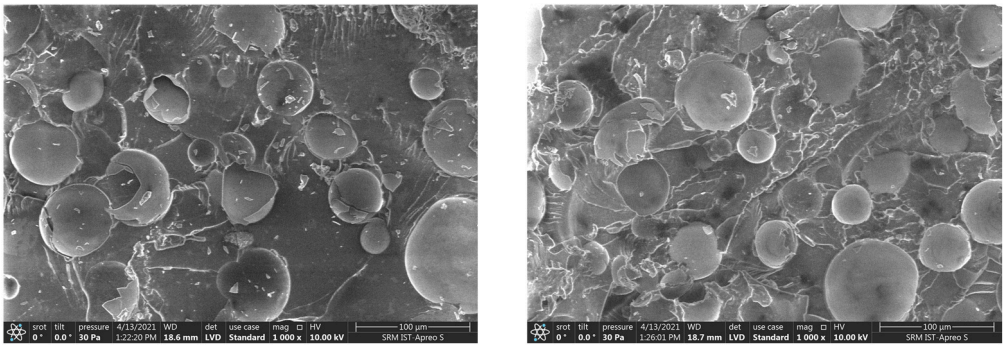


Figure 9. *Cont.*



(**e**) (**f**)

Figure 9. SEM micrographs of flexural fractured surfaces of (**a**) neat epoxy, (**b**) 2HGM/CNT/E, (**c**) 4HGM/CNT/E, (**d**) 6HGM/CNT/E, (**e**) 8HGM/CNT/E, and (**f**) 10HGM/CNT/E composite specimens.

4. Conclusions

- Fabrication and testing of thermal and mechanical properties of HGM/E, HGM/CNT/E, and HGM/G/E composites were carried out successfully.
- Tensile and flexural modulus rose with an increment in particle loading.
- Mechanical characteristics of HGM/G/E composites were found to be higher than HGM/CNT/E composites.
- The thermal conductivity of the composites reduced with the increment in weight percentage of HGM, while it increased with the rise of graphene in comparison with CNT.
- Uniform distribution of the reinforcing particles in the epoxy matrix was observed from SEM images.
- Comparing HGM/E, HGM/CNT/E, and HGM/G/E composites with varying weight percentages of HGM ranging from 0 to 10%, we found HGM/G/E composites with 10% of HGM and 0.5% of graphene by weight in epoxy matrix to be the optimum.
- The composites can be used in the fabrication of casing for energy storage devices and electronic equipment requiring dissipation of heat developed due to the chemical reaction or operation of electronic devices to the surrounding.

Author Contributions: Conceptualization, K.D. and C.V.; methodology, K.S., M.R. and V.T.; formal analysis, V.T., K.S. and M.E.M.S.; investigation, M.R., I.M.A., C.M., A.S.E.-S. and M.E.M.S.; resources, K.D. and C.M.; writing—original draft preparation, K.S. and K.D.; writing—review and editing, V.T. and I.M.A.; supervision, C.V.; funding acquisition, V.T. All authors have read and agreed to the published version of the manuscript.

Funding: The authors gratefully acknowledge the Deanship of Scientific Research, King Khalid University (KKU), Abha-Asir, Kingdom of Saudi Arabia, for funding this research work under the grant number RGP.2/58/42.

Institutional Review Board Statement: NA.

Data Availability Statement: All the data is available within the article.

Acknowledgments: The authors thank the Management and Department of Mechanical Engineering of C. Abdul Hakeem College of Engineering and Technology, Melvisharam-632509, Ranipet District, Tamil Nadu, India, for providing the facilities for the fabrication of the composites. The authors gratefully acknowledge the Deanship of Scientific Research, King Khalid University (KKU), Abha-Asir, Kingdom of Saudi Arabia, for funding this research work under the grant number RGP.2/58/42.

Conflicts of Interest: The authors declare no conflict of interest.

References

1. Jayavardhan, M.L.; Doddamani, M. Quasi-static compressive response of compression molded glass microballoon/HDPE syntactic foam. *Compos. Part B Eng.* **2018**, *149*, 165–177. [CrossRef]

2. Shahapurkar, K.; Garcia, C.D.; Doddamani, M.; Kumar, G.C.M.; Prabhakar, P. Compressive behavior of cenosphere/epoxy syntactic foams in arctic conditions. *Compos. Part B Eng.* **2018**, *135*, 253–262. [CrossRef]
3. Shahapurkar, K.; Doddamani, M.; Kumar, G.C.M.; Gupta, N. Effect of cenosphere filler surface treatment on the erosion behavior of epoxy matrix syntactic foams. *Polym. Compos.* **2019**, *40*, 2109–2118. [CrossRef]
4. Shahapurkar, K. Compressive behavior of crump rubber reinforced epoxy composites. *Polym. Compos.* **2020**, *42*, 329–341. [CrossRef]
5. Shahapurkar, K.; Chavan, V.B.; Doddamani, M.; Kumar, G.C.M. Influence of surface modification on wear behavior of fly ash cenosphere/epoxy syntactic foam. *Wear* **2018**, *414*, 327–340. [CrossRef]
6. Garcia, C.D.; Shahapurkar, K.; Doddamani, M.; Kumar, G.C.M.; Prabhakar, P. Effect of arctic environment on flexural behavior of fly ash cenosphere reinforced epoxy syntactic foams. *Compos. Part B Eng.* **2018**, *151*, 265–273. [CrossRef]
7. Gupta, N.; Woldesenbet, E.; Mensah, P. Compression properties of syntactic foams: Effect of cenosphere radius ratio and specimen aspect ratio. *Compos. Part A Appl. Sci. Manuf.* **2004**, *35*, 103–111. [CrossRef]
8. Ferreira, J.A.M.; Capela, C.; Costa, J.D. A study of the mechanical behaviour on fibre reinforced hollow microspheres hybrid composites. *Compos. Part A Appl. Sci. Manuf.* **2010**, *41*, 345–352. [CrossRef]
9. Imran, M.; Rahaman, A.; Pal, S. Carbon nano-materials coating over hollow glass microspheres and its composite foam. *Mater. Res. Express* **2019**, *6*, 125614. [CrossRef]
10. Koopman, M.; Gouadec, G.; Carlisle, K.; Chawla, K.K.; Gladysz, G. Compression testing of hollow microspheres (microballoons) to obtain mechanical properties. *Scr. Mater.* **2004**, *50*, 593–596. [CrossRef]
11. Imran, M.; Rahaman, A.; Pal, S. Effect of low concentration hollow glass microspheres on mechanical and thermomechanical properties of epoxy composites. *Polym. Compos.* **2019**, *40*, 3493–3499. [CrossRef]
12. Rahaman, A.; Imran, M. Epoxy-carbon nanotubes as matrix in glass fiber reinforced laminated composites. *Fuller. Nanotub. Carbon Nanostructures* **2017**, *25*, 559–562. [CrossRef]
13. Kim, H.S.; Khamis, M.A. Fracture and impact behaviours of hollow micro-sphere/epoxy resin composites. *Compos. Part A Appl. Sci. Manuf.* **2001**, *32*, 1311–1317. [CrossRef]
14. Yung, K.C.; Zhu, B.L.; Yue, T.M.; Xie, C.S. Preparation and properties of hollow glass microsphere-filled epoxy-matrix composites. *Compos. Sci. Technol.* **2009**, *69*, 260–264. [CrossRef]
15. Swetha, C.; Kumar, R. Quasi-static uni-axial compression behaviour of hollow glass microspheres/epoxy based syntactic foams. *Mater. Des.* **2011**, *32*, 4152–4163. [CrossRef]
16. Qiao, Y.; Wang, X.; Zhang, X.; Xing, Z. Thermal conductivity and compressive properties of hollow glass microsphere filled epoxy–matrix composites. *J. Reinf. Plast. Compos.* **2015**, *34*, 1413–1421. [CrossRef]
17. Imran, M.; Rahaman, A.; Pal, S. Thermo-Mechanical and Mechanical properties of Epoxy/CNT Composite modified by Hollow Glass Microspheres. *Mater. Today Proc.* **2020**, *22*, 2469–2474. [CrossRef]
18. Poveda, R.L.; Dorogokupets, G.; Gupta, N. Carbon nanofiber reinforced syntactic foams: Degradation mechanism for long term moisture exposure and residual compressive properties. *Polym. Degrad. Stab.* **2013**, *98*, 2041–2053. [CrossRef]
19. Lin, T.C.; Gupta, N.; Talalayev, A. Thermoanalytical characterization of epoxy matrix-glass microballoon syntactic foams. *J. Mater. Sci.* **2009**, *44*, 1520–1527. [CrossRef]
20. Mittal, G.; Dhand, V.; Rhee, K.Y.; Park, S.-J.; Lee, W.R. A review on carbon nanotubes and graphene as fillers in reinforced polymer nanocomposites. *J. Ind. Eng. Chem.* **2015**, *21*, 11–25. [CrossRef]
21. Shirodkar, N.; Ingle, A. Comparison of Mechanical and Thermal Properties of Graphene-Epoxy Nano-Composite and Epoxy Resin. *Imperial Journal of Interdisciplinary Research* **2016**, *2*, 1785–1788.
22. Kang, D.; Hwang, S.W.; Jung, B.N.; Shim, J.K. Effect of hollow glass microsphere (HGM) on the dispersion state of single-walled carbon nanotube (SWNT). *Compos. Part B Eng.* **2017**, *117*, 35–42. [CrossRef]
23. Zhao, X.; Zhang, Q.; Chen, D.; Lu, P. Enhanced mechanical properties of graphene-based poly (vinyl alcohol) composites. *Macromolecules* **2010**, *43*, 2357–2363. [CrossRef]
24. Rafiee, M.A.; Rafiee, J.; Wang, Z.; Song, H.; Yu, Z.-Z.; Koratkar, N. Enhanced mechanical properties of nanocomposites at low graphene content. *ACS Nano* **2009**, *3*, 3884–3890. [CrossRef] [PubMed]
25. Fu, S.-Y.; Feng, X.-Q.; Lauke, B.; Mai, Y.-W. Effects of particle size, particle/matrix interface adhesion and particle loading on mechanical properties of particulate–polymer composites. *Compos. Part B Eng.* **2008**, *39*, 933–961. [CrossRef]
26. Saeb, M.R.; Rabiee, N.; Seidi, F.; Far, B.F.; Bagherzadeh, M.; Lima, E.C.; Rabiee, M. Green CoNi2S4/Porphyrin Decorated Carbon-based Nanocomposites for Genetic Materials Detection. *J. Bioresour. Bioprod.* **2021**, *6*, 215–222.
27. Deeksha, B.; Sadanand, V.; Hariram, N.; Rajulu, A.V. Preparation and properties of cellulose nanocomposite fabrics with in situ generated silver nanoparticles by bioreduction method. *J. Bioresour. Bioprod.* **2021**, *6*, 75–81. [CrossRef]
28. Afolabi, O.A.; Kanny, K.; Mohan, T.P. Processing of Hollow Glass Microspheres (HGM) filled Epoxy Syntactic Foam Composites with improved Structural Characteristics. *Sci. Eng. Compos. Mater.* **2021**, *28*, 116–127. [CrossRef]
29. Park, S.-J.; Jin, F.-L.; Lee, C. Preparation and physical properties of hollow glass microspheres-reinforced epoxy matrix resins. *Mater. Sci. Eng. A* **2005**, *402*, 335–340. [CrossRef]
30. Jiang, T.; Gao, Y.; Wang, Y.; Zhao, Z.; Yu, J.; Yang, K.; Zhao, Y.; Li, W.; Wu, X. Development and Mechanical Characterization of HGMS–EHS-Reinforced Hollow Glass Bead Composites. *ACS Omega* **2020**, *5*, 6725–6737. [CrossRef] [PubMed]

31. Rahman, R.; Putra, S.Z.F.S. Tensile properties of natural and synthetic fiber-reinforced polymer composites. In *Mechanical and Physical Testing of Biocomposites, Fibre-Reinforced Composites and Hybrid Composites*; Woodhead Publishing: Cambridge, UK, 2019; pp. 81–102.
32. Gupta, N.; Nagorny, R. Tensile properties of glass microballoon-epoxy resin syntactic foams. *J. Appl. Polym. Sci.* **2006**, *102*, 1254–1261. [CrossRef]
33. Li, J.; Luo, X.; Lin, X. Preparation and characterization of hollow glass microsphere reinforced poly(butylene succinate) composites. *Mater. Des.* **2013**, *46*, 902–909. [CrossRef]
34. Shahapurkar, K.; Doddamani, M.; Kumar, G.C.M. Tensile behavior of cenosphere/epoxy syntactic foams. In *AIP Conference Proceedings*; National Institute of Technology Karnataka: Mangalura, India, 2018; Volume 1943, p. 020100.
35. Ali, I.; Kim, N.K.; Bhattacharyya, D. Effects of Graphene Nanoplatelets on Mechanical and Fire Performance of Flax Polypropylene Composites with Intumescent Flame Retardant. *Molecules* **2021**, *26*, 4094. [CrossRef]
36. El Achaby, M.; Arrakhiz, F.-E.; Vaudreuil, S.; Qaiss, A.E.; Bousmina, M.; Fassi-Fehri, O. Mechanical, thermal, and rheological properties of graphene-based polypropylene nanocomposites prepared by melt mixing. *Polym. Compos.* **2012**, *33*, 733–744. [CrossRef]
37. Stankovich, S.; Dikin, D.A.; Dommett, G.H.B.; Kohlhaas, K.M.; Zimney, E.J.; Stach, E.A.; Piner, R.D.; Nguyen, S.T.; Ruoff, R.S. Graphene-based composite materials. *Nature* **2006**, *442*, 282–286. [CrossRef]
38. Azammi, A.M.N.; Ilyas, R.A.; Sapuan, S.M.; Ibrahim, R.; Atikah, M.S.N.; Asrofi, M.; Atiqah, A. Characterization studies of biopolymeric matrix and cellulose fibres based composites related to functionalized fibre-matrix interface. In *Interfaces in Particle and Fibre Reinforced Composites*; Woodhead Publishing: Cambridge, UK, 2020; pp. 29–93.
39. Wang, F.; Drzal, L.T.; Qin, Y.; Huang, Z. Mechanical properties and thermal conductivity of graphene nanoplatelet/epoxy composites. *J. Mater. Sci.* **2015**, *50*, 1082–1093. [CrossRef]
40. Chatterjee, S.; Nafezarefi, F.; Tai, N.H.; Schlagenhauf, L.; Nüesch, F.A.; Chu, B.T.T. Size and synergy effects of nanofiller hybrids including graphene nanoplatelets and carbon nanotubes in mechanical properties of epoxy composites. *Carbon* **2012**, *50*, 5380–5386. [CrossRef]
41. Mori, T.; Tanaka, K. Average stress in matrix and average elastic energy of materials with misfitting inclusions. *Acta Metall.* **1973**, *21*, 571–574. [CrossRef]
42. Tagliavia, G.; Porfiri, M.; Gupta, N. Analysis of flexural properties of hollow-particle filled composites. *Compos. Part B Eng.* **2010**, *41*, 86–93. [CrossRef]
43. Zhu, D.; Yu, W.; Du, H.; Chen, L.; Li, Y.; Xie, H. Thermal Conductivity of Composite Materials Containing Copper Nanowires. *J. Nanomater.* **2016**, *2016*, 3089716. [CrossRef]